

RESEARCH ARTICLE | DECEMBER 04 2024

On the pressure dependence of viscosity, especially for fluids that have a tendency to form glasses

Nicholas Hopper; Rosa M. Espinosa-Marzal ; Wilfred Tysoe  

 Check for updates

J. Chem. Phys. 161, 214502 (2024)
<https://doi.org/10.1063/5.0242497>



Articles You May Be Interested In

Structure and aggregation in model tetramethylurea solutions

J. Chem. Phys. (August 2014)

Nuclear quantum effects on the high pressure melting of dense lithium

J. Chem. Phys. (February 2015)

The role of chemical order in the temperature and composition dependence of the viscosity of liquid alloys

J. Chem. Phys. (May 2019)

On the pressure dependence of viscosity, especially for fluids that have a tendency to form glasses

Cite as: *J. Chem. Phys.* **161**, 214502 (2024); doi: 10.1063/5.0242497

Submitted: 4 October 2024 • Accepted: 15 November 2024 •

Published Online: 4 December 2024



View Online



Export Citation



CrossMark

Nicholas Hopper,¹ Rosa M. Espinosa-Marzal,²  and Wilfred Tysoe^{1,3,a} 

AFFILIATIONS

¹ Department of Chemistry and Biochemistry, University of Wisconsin-Milwaukee, Milwaukee, Wisconsin 53211, USA

² Department of Materials Science and Engineering, University of Illinois Urbana-Champaign, Urbana, Illinois 61801, USA

³ Department of Physics, Universidad Nacional de San Luis, Ejercito de los Andes 950, 5700 San Luis, Argentina

^a Author to whom correspondence should be addressed: wtt@uwm.edu

ABSTRACT

Understanding fluid viscosity is crucial for applications including lubrication and chemical kinetics. A commonality of molecular models is that they describe fluid flow based on the availability of vacant space. The proposed analysis builds on Goldstein's idea that viscous transport must involve the concerted motion of a molecular ensemble, referred to as cooperatively rearranging regions (CRRs) by Adam and Gibbs in their entropy-based viscosity model for liquids close to their glass transition. The viscosity data for propylene carbonate reveal a non-monotonic trend of the activation volume with pressure, suggesting the existence of two types of CRR with different compressibility behaviors. This is proposed to result from a change in CRR free volume (<0.2 GPa) and a growth in its size (>0.2 GPa). We use Evans–Polanyi perturbation theory to develop an analytical model for the structural changes of the CRR in function of pressure and temperature and their effect on Eyring viscosity. This analysis shows that the activation energies and volumes scale with the CRR size. Using the compressibility data of propylene carbonate, we show that the activation volume of the CRR at low pressures depends on the compressibility of an ensemble comprised of the first coordination shell around a molecule. At higher pressures, we apply an Adam–Gibbs-type analysis to model the increase in CRR size and its effect on viscosity, where the increase in size is estimated from propylene carbonate's heat capacity. However, this analysis also reveals deviations from the Adam and Gibbs model that will guide future improvements.

Published under an exclusive license by AIP Publishing. <https://doi.org/10.1063/5.0242497>

I. INTRODUCTION

Of the three states of matter, the liquid is the most difficult to model because it lacks the symmetry of ideal solids but still has strong intermolecular interactions. This has meant that the molecular origins of even apparently simple phenomena such as a fluid's viscosity have remained elusive. This has technological implications. For example, understanding the way in which the viscosity of a fluid varies with pressure is important for lubrication because of the high pressures that can exist at moving contacts in machines. This has often caused quite vigorous discussions about what is the best model to use to describe the shear-rate dependences of the lubricant viscosity,^{4,5} whether it is an empirical model proposed by Carreau⁶ or a molecular-based model by Eyring,^{7,8} among others. The limitations of Eyring's molecular-based model have been thoroughly

analyzed including that this model fails to describe the high-pressure dependence of the viscosity of glass-forming liquids, which is the subject of interest of this work.⁴ A recent review has summarized the progress in the molecular-scale understanding of fluid viscosity and the ability to precisely simulate it over a wide range of pressures, shear rates, and temperatures,⁹ yet it does not discuss what are the molecular structures that are involved in the molecular-exchange processes that are required for the fluid to flow. There are also two distinct approaches to describing fluid viscosity: thermal models based on the ideas of Eyring^{7,8} and free-volume models that posit the existence of molecular voids into which molecules can move.^{10–12}

Furthermore, understanding viscous flow is intimately related to the formation of glassy materials because the increase in viscosity as the temperature is lowered prevents the molecules from

ordering into the most thermodynamically stable, crystalline states but causes them to become trapped in a metastable “glassy” configuration.¹³ Here, the theory focuses on the viscous properties as the fluid approaches the glass-transition temperature, while understanding the rheological properties over a wide range of temperatures and pressures is required for technological applications. It is a theoretical challenge to unify the behavior in both regimes, and this is the essence of the problem addressed here. This is arguably due to the limited understanding of the molecular structures involved in molecular motion in a fluid and the models to analyze them.

Goldstein suggested that thermal models should provide the most promising approach for analyzing viscosity,¹³ as long as the energy barriers were greater than $k_B T$. He also argued, by analogy with Orowan’s analysis of dislocation motion,¹⁴ that viscous molecular transport must involve the concerted motion of an ensemble of molecules. This is referred to as a cooperatively rearranging region (CRR) by Adam and Gibbs.¹⁵

The first models suggested by Eyring involved a molecule moving into some vacant site (with some free volume, V_f) as shown in Fig. 1(a), but there were clear objections to this model as, for example, pointed out by Alfrey.¹⁶ The first is that this model cannot lead to molecules moving large distances, and, second, such a lateral translation would not be induced by shear stresses. Alfrey proposed an alternative process [Fig. 1(b)] in which two molecules change places, thus causing a net molecular motion, analogous to the Grotthuss mechanism for proton transport through water,¹⁶ although Eyring did later propose similar models.¹⁷ Group-theoretical considerations suggest that the symmetry of the molecular motion should be the same as that of the perturbation that induces it (here, a shear), in support of such a model. Here, the energy barrier is due to an interaction of a molecular dimer with the surroundings to provide the space to allow molecular exchange to occur. A more plausible model that does not need to postulate the existence of such a special dimeric configuration is shown in Fig. 1(c) (Robert Thomas, Oxford University, personal communication), which resembles the Alfrey model except that it involves an exchange between a molecule and another neighboring molecule in the first coordination sphere.

Assuming that the central blue molecule can only exchange with adjacent neighboring molecules, the number of molecules in this ensemble is $1 + \bar{n}_{nn}$, where \bar{n}_{nn} is the average number of molecules in the first coordination sphere. There are, on average, ~12 molecules in the first coordination sphere of a liquid so that the number of molecules in the ensemble is ~13. The number of molecules in the two-dimensional slice shown in the cartoon in Fig. 1(c) is ~7.

Such a simple, single ensemble suggests that there should be an exponential dependence of viscosity on hydrostatic pressure P , $\eta = \eta_0 \exp(\alpha_B P)$, where η is the viscosity, as proposed by Barus,¹⁸ and α_B is a Barus constant. Figure 2 shows a plot of $\log(\eta)$ vs P for propylene carbonate, a well-known glass-forming fluid, which should be linear if the Barus equation were obeyed. There are clear deviations from linearity, in particular at lower temperatures. The following work addresses the origins of these deviations from linearity and will focus on propylene carbonate because other properties of this fluid that are relevant to the analysis of its viscous behavior have been measured. It also has technological applications as an electrolyte for Li-ion batteries,¹⁹ where viscosity²⁰ and dielectric constant²¹ are important properties of battery electrolytes. Such deviations from linearity are commonly observed for molecular fluids.^{22,23}

To analyze this molecular model using an Eyring-type approach, we use a perturbation method of transition-state theory proposed by Evans and Polanyi^{24–26} to analyze the effect of stresses on the rates of chemical reactions.^{27–31} This method allows activation volumes to be calculated for several simultaneous perturbations such as combined normal and shear stresses^{30,32} and is therefore ideally suited to analyzing the molecular origins of viscosity.

Such analyses have also found that the activation volumes can themselves depend on pressure due to the compression of the reactant and transition-state structures,^{31,33} and it is anticipated that similar higher-order effects will operate on the ensembles that facilitate molecular exchange. While many analyses of fluid properties such as liquid–solid equilibria treat them as incompressible, they do compress, especially under the influence of high pressures in the GPa range (~10 000 atm). The isothermal compressibility, $\kappa_T = -\frac{1}{V} \frac{\partial V}{\partial P}|_T$ vs the hydrostatic pressure of a glass-forming fluid, propylene

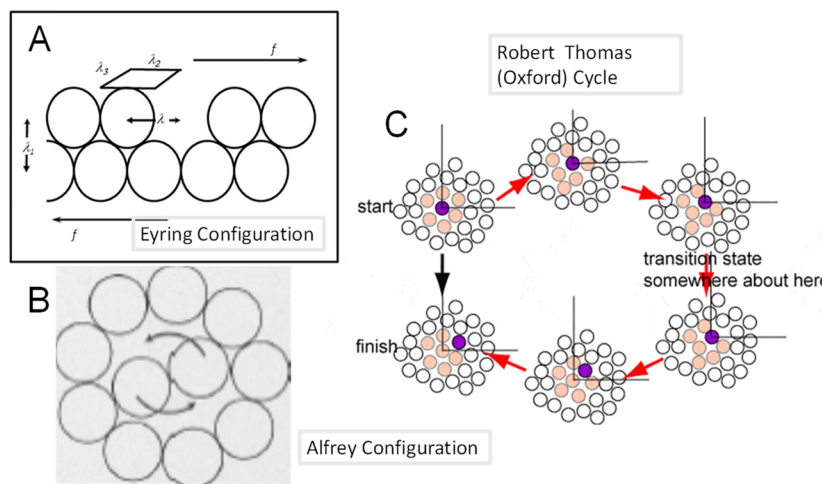


FIG. 1. Possible depictions of the assemblies proposed by (a) Eyring and (b) Alfrey and (c) a cartoon showing snapshots of the evolution of a proposed molecular assembly in a fluid that leads to molecular exchange and transport.

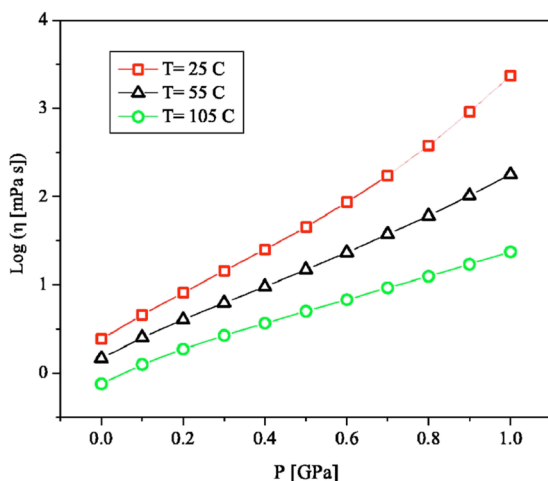


FIG. 2. Pressure dependence of the viscosity of propylene carbonate for various temperatures. Reproduced with permission from R. Casalini and S. Bair, *J. Chem. Phys.* **128**, 084511 (2008). Copyright 2008 AIP Publishing LLC.

carbonate, for which the viscosity is shown in Fig. 2, is displayed in Fig. 3. The fluid becomes less compressible as the pressure increases. The general features of this behavior can be understood using the structural depictions in Fig. 1(c), where, above the melting temperature, $k_B T > U_{int}$, in which U_{int} is the interaction potential of the fluid, the behavior is dominated by the weak intermolecular van der Waals' interactions. At low pressures, the molecules oscillate about some average intermolecular spacing with an amplitude, x , where the average potential energy is given by $\langle U \rangle = \frac{1}{2}k\langle x \rangle^2$. Here, k is a

harmonic force constant between adjacent molecules in the fluid and $\langle x^2 \rangle$ is the mean-square displacement from the equilibrium position. Note that the average displacement $\langle x \rangle$ is, by definition, zero in the absence of fluid shear. From the equipartition of energy, the average energy equals $\frac{1}{2}k_B T$ so that the mean-square displacement $\langle x \rangle^2 = \frac{k_B T}{k}$. A statistical thermodynamic analysis of fluid compressibility indicates that it depends on the fluctuations in particle density,³⁴ which is expected to increase with increasing temperature in accord with the data in Fig. 3. An increase in mean-square displacement of the molecules will result in an increase in the free volume, the volume of the system that is not occupied in the van der Waals' cocoon surrounding each molecule.^{35,36}

At higher pressures, the molecules in the fluid become closer to each other so that their van der Waals' surfaces eventually come into contact and the compressibility becomes relatively temperature independent. This suggests that variations in pressure dependence can be divided into two regimes: one below ~ 0.2 – 0.3 GPa for the fluid shown in Fig. 3 (propylene carbonate), where the temperature-dependent compressibility decreases with pressure because the vibrational amplitudes decrease with increasing pressure.

The second regime occurs at pressures above ~ 0.2 – 0.3 GPa, where the molecules come into contact and the compressibility is controlled by the Pauli repulsion between them. As we shall see below, this transition correlates with changes in viscous properties (see Fig. 4). Interestingly, despite the different physical origins of the compressibility at low and high pressures, the experimental data are well reproduced by a single Tait equation³⁷ over the whole pressure range.

Traditionally, the Eyring viscosity model is derived in terms of just the shear stress^{7,8} and the pressure dependence of the viscosity is added later in *ad hoc* fashion. This has meant that it is difficult to attribute a physical meaning to the pressure-dependent activation

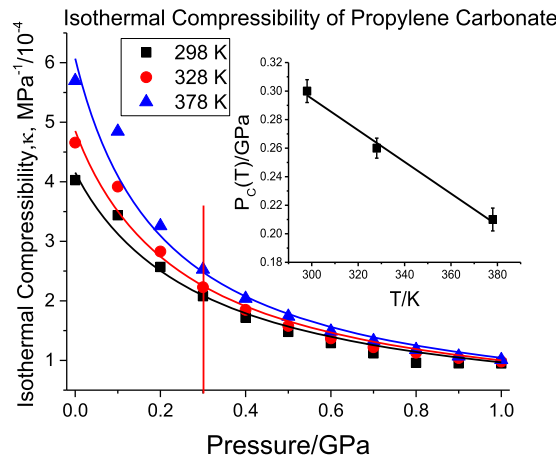


FIG. 3. Plot of the isothermal compressibility taken from Casalini and Bair of propylene carbonate at several temperatures as a function of pressure up to a maximum value of 1 GPa. The lines are fits to the Tait equation, $\kappa_T = \frac{c}{P_c(T) + P}$. Reproduced with permission from S. Pawlus *et al.*, *Phys. Rev. E* **70**, 061501 (2004). Copyright 2024 American Physical Society.²

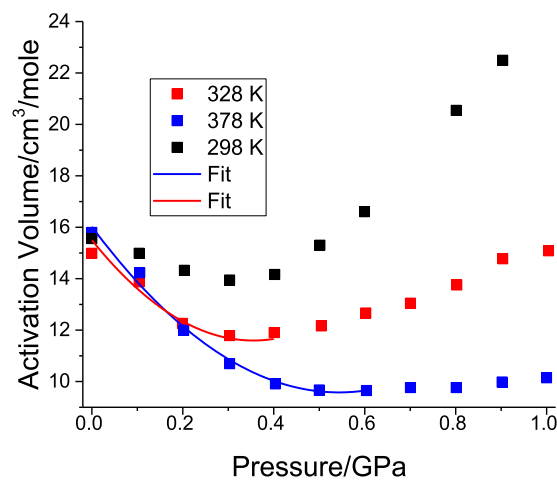


FIG. 4. Variation in the viscosity activation volume as a function of pressure for different fluid temperatures. The values of the activation volume were obtained from $\Delta V^\ddagger = \frac{\partial \ln \eta}{\partial P} \Big|_T$ from the measured viscosity from Fig. 2. The solid lines show second-order fits to the data collected at 328 and 378 K. Reproduced with permission from R. Casalini and S. Bair, *J. Chem. Phys.* **128**, 084511 (2008). Copyright 2008 AIP Publishing LLC.

volume. We will use Evans–Polanyi perturbation theory to derive an equation for the pressure-dependent Eyring viscosity. The goal of this work is thus to postulate elementary-step processes that occur in fluid shear such as shown in Fig. 1(c) and use Evans–Polanyi theory to analyze the pressure-dependent viscosity to be able to rationalize the experimental results.

Based on the structures discussed above [Fig. 1(c)], we first briefly summarize the ideas behind Evans–Polanyi (E–P) theory. We then describe the molecular ensembles that can facilitate molecular exchange. Note that we will focus here on molecules, not on segments of polymers, although the analysis in that case may be similar. Next, we show how the E–P analysis can be used to analyze fluid viscosity within the framework of an Eyring-type model. The analysis will first be carried out for pressure/stress-independent activation volumes and then be extended to include effects in which the activation volumes are influenced by the pressure. Finally, we will extend the analysis to glass-forming liquids where the size of the reacting assembly, the cooperatively rearranging regions (CRRs), varies with temperature and pressure,¹⁵ to allow the pressure- and shear-dependent kinetics also to be analyzed by E–P theory.

II. OUTLINE OF EVANS–POLANYI THEORY

The Evans–Polanyi analysis is based on the idea that the equilibrium constant of a chemical reaction, K , can be obtained from the standard Gibbs free energy change per mole for the process, ΔG^0 , as

$$\Delta G^0 = -RT \ln K, \quad (1)$$

where R is the gas constant and T is the absolute temperature.³⁸ For an isobaric system, $\Delta G = \Delta U + P\Delta V - T\Delta S$, the variation in equilibrium constant with (hydrostatic) pressure is given by $\frac{\partial \ln K}{\partial P} \Big|_T = -\frac{\Delta V}{RT}$, where ΔV has the units of volume per mole; it corresponds to a difference in molar volumes between the reactants and the products. Evans and Polanyi argued that, rather than using statistical thermodynamics to calculate the equilibrium constant between the transition state and the reactant,³⁹ classical thermodynamic concepts could be used instead. As a result, a similar equation could be written for a rate constant k as $\frac{\partial \ln k}{\partial P} \Big|_T = -\frac{\Delta V^\ddagger}{RT}$, where ΔV^\ddagger is a molar activation volume. If the rate constant under a standard pressure is k_0 , then $k(P) = k_0 \exp\left(-\frac{P\Delta V^\ddagger}{RT}\right)$. This has been called the Bell equation in chemistry⁴⁰ but was originally applied to analyzing cell adhesion. Using the Arrhenius form of the rate constants shows that $E_{act}(P) = E_{act}^0 + P\Delta V^\ddagger$, where E_{act}^0 is the activation barrier in the absence of an applied pressure and $E_{act}(P)$ is the pressure-dependent barrier. Thus, a decrease in the volume of the activated complex relative to the reactant causes ΔV^\ddagger to be negative so that increasing the pressure reduces the activation barrier and increases the rate. The pressure sensitivity of the rate of a process depends on the ratio $E_{act}^0/\Delta V^\ddagger$, where processes with lower activation barriers (such as viscous flow) will be more sensitive to a volume change between the initial and transition states than a chemical reaction, where the activation energies are much higher, but the magnitude of the activation volumes is similar.^{41,42}

There are several advantages to using such an approach compared to those, for example, that use a force-modified potential energy surface.^{43,44} First, as a consequence of Hess' law,³⁸ this analysis does not depend on the pathway between the activated

complex and the reactant.⁴⁵ This provides a significant advantage for applications to real systems, because calculating the potential-energy surface is tedious, while obtaining just the reactant and transition-state energies and structures and their properties is much simpler.^{46–49} Second, the Evans–Polanyi perturbation model can easily be extended to describing the effect of a combination of stresses as well as including the effects of other perturbations. This approach facilitates linking macroscale sliding phenomena to the molecular origins that underpin them.

Thus, the central concept behind Evans–Polanyi (E–P) perturbation theory is that the Gibbs free energy of a system can include the influence of any perturbations described by an intensive variable, I (e.g., hydrostatic pressure or shear stress), by using an associated, extensive conjugate variable C , where $I dC$ equals the reversible work, so that $G = U - TS + IC$.⁵⁰ Note that the value of the conjugate variable, C , can itself depend on I ,^{24,25} so that the equation for the standard Gibbs free energy change becomes

$$\Delta G^0 = \Delta U^0 - T\Delta S^0 + I\Delta C^0(I). \quad (2)$$

$\Delta C^0(I)$ can most conveniently be evaluated by carrying out a Taylor-series expansion in I . The resulting rate constant k is given by

$$\ln K(I) = \ln k_0 - \frac{\Delta C^\ddagger(I)}{RT} I, \quad (3)$$

where again k_0 is the rate constant for the process in the absence of the perturbation.

III. NATURE OF THE MOLECULAR ENSEMBLES IN A FLUID THAT ARE RESPONSIBLE FOR MOLECULAR MOTION

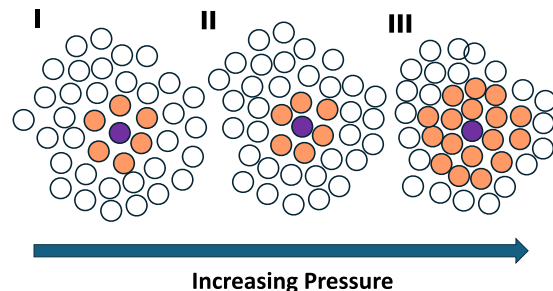
The central assumption behind the Eyring viscosity model is that molecular motion is a thermally activated process for which the activation barrier is modified by the stress. Eyring initially proposed a process such as that depicted in Fig. 1(a), where a molecule diffuses into a vacant site. There are clear objections to this model as pointed out by Alfrey,¹⁶ who proposed an alternative configuration [Fig. 1(b)] in which two molecules change place, thus causing a net motion of the molecule. A similar model to that proposed by Alfrey is depicted in Fig. 1(c) (Robert Thomas, Oxford University, personal communication) except that, here, exchange occurs between a molecule at the center of a cluster of surrounding molecules and one of its nearest neighbors. This model, being simpler than that suggested by Alfrey, seems more plausible because it does not require the creation of some special dimeric species. Figure 1(c) shows a two-dimensional depiction of a three-dimensional cluster, and this model assumes that the shear stresses are aligned in the plane of this figure.

To more clearly define the various pressure-dependent viscosity regimes, the viscosity results shown in Fig. 2 were analyzed to yield pressure-dependent activation volumes, $\Delta V^\ddagger(P) = \frac{\partial \ln \eta}{\partial P} \Big|_T$, which are plotted vs pressure in Fig. 4. The activation volumes at zero stress are $\sim 15 \text{ cm}^3/\text{mol}$ ($\sim 26 \text{ \AA}^3/\text{molecule}$) for all temperatures and are of the same order of magnitude as for chemical reactions. However, the behavior at higher pressures depends on the temperature. The activation volume first decreases with increasing pressure up to 0.3–0.5 GPa and then increases at higher pressures, only slowly

at 378 K, but much more rapidly at 298 K, while the change at 328 K is intermediate between that at 298 and 378 K so that the inflection point depends on temperature. Such a behavior for glass-forming liquids was first reported by Bridgman⁵² and later by others (e.g., Refs. 51 and 53).

An Eyring viscosity analysis (see below) assumes that there is a single energy barrier for the process, and this results in an Arrhenius-type temperature dependence of the viscosity. This has been seen experimentally, thereby implying that there is indeed a single structure that leads to molecular motion. However, a different temperature-dependence has been observed for glass-forming liquids in which the viscosity varies with temperature as $\eta = A \exp\left(\frac{B}{T-T_0}\right)$, where A and B are constants, known as the Vogel–Fulcher–Tammann (VFT) model,^{54–56} where T is the absolute temperature and T_0 is a reference temperature known as the Vogel temperature. This equation can also be derived from the Doolittle equation^{35,36} by assuming a simple model for the amount of free volume in the liquid and glass that enables the molecule to move, as shown in Fig. 1(c).^{11,57} The Doolittle equation (originally used to fit the viscosity of *n*-alkanes) gives $\eta = A \exp\left(\frac{BV_0}{V_f}\right)$, where V_0 is the volume of the fluid occupied by the molecules and $V_f = V - V_0$, is the free volume, and $V = V(T)$, the specific volume at temperature T . This model assumes that the barrier for motion is of an entropic nature and, in comparison, the energy barrier is small. If $T_0 \rightarrow 0$, the expression reduces to an Arrhenius-type dependence of the viscosity; experimentally, it is found that $T_0 > 0$ K, but below the experimentally measurable glass transition temperature, T_g .

A different model has ascribed this temperature-dependence of the viscosity to a decrease in the structural entropy as the temperature approaches a second-order (liquid–solid) phase transition. The enhanced entropic barrier reduces the transition rate, thereby trapping the system in a metastable glassy state, which hinders the system from reaching the second-order phase transition temperature. Adam and Gibbs analyzed this behavior¹⁵ and postulated a cooperatively rearranging region (CRR) where the size of the CRR increases as the temperature decreases toward the glass-transition temperature. This implies that the molecular ensemble/CRR varies depending on the conditions (temperature and pressure) to account for the complex behavior highlighted in Figs. 2 and 4. There have been a number of proposals concerning the nature of the CRRs⁵⁸ that have led to widely varying estimates of shape and size of the CRR.⁵⁹ Clearly, its size varies depending on the conditions, and an analysis of the pressure-dependent viscosity behavior as a function of temperature can provide insights into the nature of the CRR. A proposed molecular model for the behavior is outlined in Fig. 5. At low pressures, the structure of the exchanging ensemble does not change because there is sufficient space (free volume) for two (blue and orange) molecules to exchange. As the pressure increases, the ensemble is compressed to decrease the average inter-molecular separation until the molecules become so close that exchange with nearest-neighbor molecules cannot occur directly (when it forms ensemble II). Here, enough space for the exchange within the ensemble can only be made by molecules moving farther from the center of the ensemble. This requires the size of the ensemble to increase as shown in ensemble III so that the inflection point in the plot of activation volume with pressure (Fig. 4) coincides with the



Increasing Pressure

FIG. 5. Cartoons of the proposed variation in the ensembles that allow motion of a molecule to an adjacent site as a function of pressure. Ensemble I is that shown in Fig. 1(c), where the blue atom can move by only the orange atoms moving to change places with one of the adjacent molecules. As the pressure increases, the volume of the ensemble decreases to reduce the free volume (ensemble II), but still leaves sufficient space for a blue molecule to exchange with an orange one. As the pressure increases further, the molecules become closer to each other (ensemble III) so that a blue molecule can no longer exchange with an orange one without additional molecules, also indicated in orange, moving out of the way. This leads to the formation of larger CRRs at high pressures and low temperatures.

formation of ensemble II; the temperature-dependent change in inflection point reflects how the transition from ensemble I to ensemble II depends on temperature. Thus, while only a molecule in the center of the ensemble can exchange with a nearest neighbor, to accomplish this in more-compressed systems requires a larger number of other molecules to move to make space for this process to occur. This is the cooperatively rearranging region (CRR) referred to by Adam and Gibbs. It should be emphasized that this picture is in general accord with the free-volume concept where the free volume V_f is the total free volume of the whole ensemble/CRR. As the pressure increases, the total number of molecules in the ensemble has to increase to create the same total free volume, V_f . A similar idea has also been suggested by Powell *et al.*⁶⁰ The way in which these concepts are applied will be outlined using E–P theory as indicated below.

IV. MOLECULAR-EXCHANGE KINETICS IN A COOPERATIVELY REARRANGING REGION CALCULATED USING EVANS–POLANYI THEORY

The E–P analysis of the Eyring model of fluid viscosity is modified to take account of the postulate that the reacting ensemble (or CRR) must comprise a minimum number of molecules [Fig. 1(c)] where, following Adam and Gibbs, we will calculate an isobaric rate constant $k(P, T)$ and then include a shear stress as a perturbation using E–P theory. The viscosity, η , is defined as the ratio of shear stress to shear rate, $\frac{dy}{dt} = \dot{\gamma}$, so that $\eta = \frac{\tau}{\dot{\gamma}}$. The shear rate, defined by Eyring in terms of molecular processes, is given by $\dot{\gamma} = \frac{\Delta v}{d}$, where d is the spacing between the sheared molecular layers and Δv is the velocity difference between them. If the rate constant for motion in the forward (i.e., along the shear) direction is k_f and along the reverse direction is k_r , then $\Delta v = \Delta x^{\ddagger}(k_f - k_r)$, where Δx^{\ddagger} (an activation length) is the distance from the initial state to the transition state along the shearing direction. Because the initial and final configurations of the exchange processes are identical,

the activation lengths for the forward and reverse processes are also identical. Thus, if the lateral distance moved by a molecule during this exchange process is a , then $\Delta x^\ddagger = \frac{a}{2}$. If, as shown in Fig. 1(c), this involves a (blue) molecule moving from the center of the cluster to a position in the adjacent shell (an orange molecule), a corresponds approximately to an intermolecular spacing. This structure is also shown as ensemble I in Fig. 5.

Within the context of the structural model shown in Fig. 1(c) (and ensemble I in Fig. 5), the pressure dependence of the structural evolution that allows molecular exchange to occur is depicted in Fig. 5 in going from ensembles I through II to III. We first investigate the low-pressure behavior in which only structure I is present. The effect of the evolution to larger CRRs will be addressed using a modified Adam–Gibbs theory in Sec. VII.

We take an isobaric, single-particle partition function of a system with a series of energy levels, ϵ_i , and average volume occupied by each molecule V_i to be

$$z(T, P) = \sum_{\epsilon_i, V_i} w(\epsilon_i, V_i) \exp(-\epsilon_i/k_B T) \exp(-PV_i/k_B T), \quad (4)$$

where P is the pressure, T is the temperature, k_B is the Boltzmann constant, and w are the degeneracies of the levels. This is formally applicable to non-interacting or weakly interacting molecules, while glass formation and solidification will involve strong intermolecular interactions, which could be estimated, for example, using a configuration integral.⁶¹ The N particle partition function is obtained for indistinguishable particles where the molecular motion is assumed to be localized so that there is no translational contribution to the partition function and gives $Z(T, P, N) = \frac{z(T)^N}{N!} \exp(-PV/k_B T)$, where $V = NV_i$. Using Stirling's approximation, this yields a value of $\ln Z(T, P, N) = N \ln z(T) - N \ln N - N - \frac{PV}{k_B T}$. The chemical potential μ for this weakly interacting system is given by $\mu = -k_B T \frac{\partial \ln Z}{\partial N} \Big|_{T, P}$. If the average volume of the ensembles equals \tilde{V} , this yields the chemical potential as $\mu = -k_B T (\ln Z(T) - \ln N) + P\tilde{V}$, where the first term is the vibrational contribution, the second is the configurational contribution, and the last is the work done on the system.

From above, and following the Adam–Gibbs analysis, we are interested in calculating the rate of exchange of two molecules in an ensemble containing α molecules that can, in principle, vary with the temperature and pressure. We will initially assume that the pressures are sufficiently low that this “CRR” corresponds to ensemble I in Fig. 5, where α remains constant with an increase in pressure and a decrease in temperature. In order to accomplish this, we will calculate a pressure-dependent molecular-exchange rate using E–P theory from the difference in Gibbs free energies between the transition- and initial-states of this ensemble using Eq. (3) to calculate $k(T, P)$. We will then use this rate constant to calculate an Eyring viscosity, again using the E–P model.

If we take the common energy reference of the ensemble of α molecules to be that of the ground-state (initial) configuration, then its chemical potential μ_I is given by

$$\mu_I = -k_B T \left(\ln \left(\frac{z_I(T)}{\alpha} \right) - \frac{P\tilde{V}_I}{k_B T} \right), \quad (5)$$

where \tilde{V}_I is the average volume per molecule in the initial configuration. A similar equation can be written for the transition-state configuration, which has an average energy per molecule, E^\ddagger , relative to the ground state, with an average volume per molecule, \tilde{V}_T , to give a transition-state partition function,

$$\mu_T = -k_B T \left(\ln \left(\frac{z_T(T)}{\alpha} \right) - \frac{E^\ddagger}{k_B T} - \frac{P\tilde{V}_T}{k_B T} \right). \quad (6)$$

Thus, following Adam–Gibbs, $\Delta G = \alpha(\mu_T - \mu_I)$, and the hydrostatic-pressure-dependent rate constant $k(T, P)$ is obtained according to E–P theory from $\Delta G = -k_B T \ln(k(T, P))$ as

$$k(T, P, \alpha) = v_T \left(\frac{z_T(T)}{z_I(T)} \right)^\alpha \exp \left(-\frac{\alpha E^\ddagger}{k_B T} \right) \exp \left(-\frac{\alpha P \Delta V^\ddagger}{k_B T} \right), \quad (7)$$

where $\tilde{V}_T - \tilde{V}_I = \Delta V_p^\ddagger$ is the average pressure-dependent volume difference per molecule between the initial- and transition-state structures and v_T is the vibrational frequency of the (frustrated) rotational mode of the transition-state structure that leads it to decaying to the initial state. Assuming that the frequencies of the skeletal vibrational modes of the molecule are sufficiently high that their partition functions are close to unity gives $z(T) \cong \prod_i \frac{k_B T}{\hbar \omega_i}$, where ω_i are the angular frequencies for the low-frequency frustrated translational and rotational modes of each molecule. This yields $z_T(T) = \frac{k_B T}{\hbar} \prod_{R^T, T^T} \frac{1}{\omega_{R^T, T^T}}$, where R^T and T^T label the frustrated rotational and translational modes of the transition-state ensemble and $z_I(T) = \frac{k_B T}{\hbar} \prod_{R^I, T^I} \frac{1}{\omega_{R^I, T^I}}$ is the corresponding formula of the initial-state ensemble. Since the low-frequency vibrations of the initial- and transition-state structures are likely to be similar, $\left(\frac{z_T(T)}{z_I(T)} \right) \sim 1$, and this implies that the intrinsic exchange rate, $\bar{k}_0 = v_T \left(\frac{z_T(T)}{z_I(T)} \right)^\alpha$, in Eq. (7) should be a constant value close to v_T , as proposed by Adam and Gibbs.¹⁵

Adam–Gibbs assumed that there is a minimum number of molecules, α^* , in the ensemble/CRR that allow molecular exchange to occur, as shown in Fig. 5. The total exchange rate for all allowed molecular ensembles, $\bar{k}(T, P)$, is given by

$$\bar{k}(T, P) = \sum_{\alpha^*}^{\infty} \bar{k}_0 \left[\exp \left(-\frac{(E^\ddagger + P \Delta V^\ddagger)}{k_B T} \right) \right]^\alpha, \quad (8)$$

assuming that $\bar{k}(T, P) = 0$ for $\alpha < \alpha^*$. Since the exponential term is less than unity, the infinite series converges and yields a rate constant $\bar{k}(T, P) = \frac{\bar{k}_0}{\left(1 - \exp \left(-\frac{(E^\ddagger + P \Delta V^\ddagger)}{k_B T} \right) \right)} \exp \left(-\frac{\alpha^* (E^\ddagger + P \Delta V^\ddagger)}{k_B T} \right)$. In general, $\frac{(E^\ddagger + P \Delta V^\ddagger)}{k_B T}$ should be quite large so that its exponential is much less than 1 so that Eq. (8) becomes

$$\bar{k}(T, P) = \bar{k}_0 \exp \left(-\frac{\alpha^* (E^\ddagger + P \Delta V^\ddagger)}{k_B T} \right). \quad (9)$$

This formula is less accurate for processes with low activation barriers.⁶² This suggests that, for processes with sufficiently high

activation barriers, the rate will be dominated by an ensemble with a single number of α^* molecular components with a single activation energy given by $\alpha^* E^\ddagger$ and an activation volume of $\alpha^* \Delta V^\ddagger$ and is consistent with the assumptions made in Eyring theory. This has recently been verified in simulations using just a single barrier that yield good agreement with experimental results.⁶³

V. SHEAR STRESS AS PERTURBATION

As shown previously,³⁰ the molar Gibbs free energy change between the transition-state and the initial-state under the influence of a shear stress τ is given by $G = \Delta U - T\Delta S + P\alpha^* \Delta V_P^\ddagger + \tau\alpha^* \Delta V_S^\ddagger$, where ΔV_S^\ddagger is the activation volume per molecule along the x (shear) direction. Thus, ΔV_P^\ddagger is the isotropic volume difference between the transition- and initial-state ensemble (CRR) configurations, while ΔV_S^\ddagger is the volume difference along the shearing direction, which are the volume changes conjugate to hydrostatic pressure and shear stress, respectively. Using Evans and Polanyi perturbation theory^{24,25} gives $\frac{\partial \ln(k(\tau))}{\partial \tau} \Big|_{T,P} = -\frac{\alpha^* \Delta V_S^\ddagger}{k_B T}$ to yield formulas for the forward and reverse rate constants under the influence of a shear stress as

$$\bar{k}_f(\tau, P, T) = \bar{k}(T, P) \exp\left(-\frac{\alpha^* \Delta V_S^\ddagger \tau}{k_B T}\right), \quad (10)$$

$$\bar{k}_r(\tau, P, T) = \bar{k}(T, P) \exp\left(-\frac{(-\alpha^* \Delta V_S^\ddagger \tau)}{k_B T}\right), \quad (11)$$

where $\bar{k}(T, P)$ is the pressure-dependent rate constant [Eq. (9)] and ΔV_S^\ddagger is assumed to be independent of τ . Note that ΔV_S^\ddagger must be negative for the forward transition rate to increase in a direction aligned with the shear force. These rate equations can be substituted into the equation for the velocity gradient to give

$$\Delta v = \Delta x^\ddagger \bar{k}(T, P) \left\{ \exp\left(-\frac{\alpha^* \Delta V_S^\ddagger \tau}{k_B T}\right) - \exp\left(-\frac{(-\alpha^* \Delta V_S^\ddagger \tau)}{k_B T}\right) \right\}. \quad (12)$$

This can be simplified by rearranging and substituting for Δv to give an equation of the shear rate as follows:

$$\dot{\gamma} = \frac{2\bar{k}(T, P) \Delta V_S^\ddagger}{A_C d} \sinh\left(-\frac{\alpha^* \Delta V_S^\ddagger \tau}{k_B T}\right), \quad (13)$$

where using the Stearn–Eyring approximation⁶⁴ gives $\Delta V_S^\ddagger = \Delta x^\ddagger A_C$, in which A_C is the area over which the stress acts. This yields a pressure-dependent Eyring viscosity, $\eta_e = \tau/\dot{\gamma}$,

$$\eta_e = \frac{\tau A_C d}{2\bar{k}(T) \Delta V_S^\ddagger} \frac{\exp\left(\frac{P\alpha^* \Delta V_P^\ddagger}{k_B T}\right)}{\sinh\left(-\frac{\alpha^* \Delta V_S^\ddagger \tau}{k_B T}\right)}, \quad (14)$$

where $\bar{k}(T) = \bar{k}_0 \exp\left(-\frac{\alpha^* E^\ddagger}{k_B T}\right)$, which is a constant as long as the number of molecules in ensemble I (with α^* molecules) remains constant. Here, the pressure-dependent activation volume, ΔV_P^\ddagger , is positive, that is, the volume of the transition-state structure must

be larger than that of the initial state to cause the viscosity to increase with pressure (Fig. 2). This is in accord with the cartoon shown in Fig. 1(c), where the intermolecular distance decreases along the shear direction as molecular exchange occurs, while the total volume of the ensemble increases. This formula is identical to that derived by Eyring^{8,65} except for an additional pressure term $\exp\left(\frac{P\alpha^* \Delta V_P^\ddagger}{k_B T}\right)$, known as the Barus equation,¹⁸ where $\alpha_B(T) = \frac{\alpha^* \Delta V_P^\ddagger}{k_B T}$ is the Barus pressure–viscosity coefficient. This has previously been derived as a separate equation but arises here quite naturally using an Evans–Polanyi analysis. Assuming that $\alpha^* \sim 13$, the zero-pressure activation volume is $\alpha^* \Delta V_P^\ddagger = 15.5 \text{ cm}^3/\text{mol}$ ($\sim 25 \text{ \AA}^3/\text{molecule}$, Fig. 4). The molar volume of propylene carbonate is $87 \text{ cm}^3/\text{mol}$ ($\sim 145 \text{ \AA}^3/\text{molecule}$) at 298 K so that an ensemble with $\alpha^* = 13$ molecules has a total volume of $V_o \sim 13 \times 145 = 1885 \text{ \AA}^3$ so that, if we assume that V_f is the minimum volume required for molecular exchange to occur, and $V_f \sim \alpha^* \Delta V_P^\ddagger$, the free-volume fraction is $\frac{V_f}{V_o} \sim 0.02$, which is in the range of free-volume fractions for organic liquids.⁶⁶

The Eyring viscosity depends on the pressure and shear stress, while the Newtonian viscosity η_n is a material property and is independent of the stress. This occurs as the stresses tend to zero so that $\exp\left(-\frac{\alpha^* \Delta V_P^\ddagger P}{k_B T}\right) \rightarrow 1$ as $P \rightarrow 0$ and $\sinh\left(-\frac{\alpha^* \Delta V_S^\ddagger \tau}{k_B T}\right) \rightarrow -\frac{\Delta V_S^\ddagger \tau}{k_B T}$ as $\tau \rightarrow 0$ to give a Newtonian viscosity, $\eta_n = \frac{k_B T A_C d}{2\bar{k}(T) (\alpha^* \Delta V_S^\ddagger)^2}$, which depends on the material and the temperature. If we define an Eyring stress as $\tau_e = \frac{k_B T}{\alpha^* \Delta V_S^\ddagger}$, the strain rate is given by

$$\dot{\gamma} = \frac{\tau_e}{\eta_n} \exp(\alpha_B(T)P) \sinh\left(-\frac{\tau}{\tau_e}\right), \quad (15)$$

which is used to model shear-thinning of lubricants under severe conditions of pressure and stress. The Eyring stress is taken to define the stress at which there is a transition from the Newtonian behavior to shear-thinning described by an Eyring viscosity. Eyring stresses are the order of 10 MPa for a typical lubricant fluid.^{67,68} As described in Ref. 4, Eyring's model is not able to account for the inflection point of the viscosity of glass-forming liquids, among other shortcomings, that have led to various modifications in the past.⁶⁷ Note that the pressure-dependent Eyring viscosity obtained here [Eq. (14)] accounts for a varying activation volume to eventually be able to model the inflection point in the viscosity-vs-pressure results.

The above analysis also assumes that the activation volumes themselves do not depend on pressure. However, as ensemble I is compressed to form ensemble II (Fig. 5), the values of the activation volumes, $\alpha^* \Delta V_S^\ddagger$, and the Barus coefficient $\alpha_B(T, P) = \frac{\alpha^* \Delta V_P^\ddagger}{k_B T}$ are expected to change. This will be discussed in Sec. VI.

VI. INFLUENCE OF SHEAR STRESS/PRESSURE-DEPENDENT ACTIVATION VOLUMES ON THE EYRING VISCOSITY

Now, we consider the possibility that the activation volume itself can depend on the hydrostatic pressure, $\Delta V_P^\ddagger(P)$, so that the pressure-dependent rate constant is

$\bar{k}(T, P) = \bar{k}_0 \exp\left(-\frac{\alpha^*(E^\ddagger + P\Delta V_P^\ddagger(P))}{k_B T}\right) = \bar{k}_0(T) \exp(\alpha_B(T, P)P)$, to indicate the possibility that the Barus coefficient, $\alpha_B(T, P)$, can depend on pressure. The pressure dependence of the activation volume will depend on the isothermal compressibility of the fluid, which is given by the Tait equation: $\kappa_T = -\frac{1}{V} \frac{\partial V}{\partial P}|_T = \frac{C}{P_C(T) + P}$, where $P_C(T)$ is a temperature-dependent reference pressure, and both C and $P_C(T)$ are known parameters for a fluid. The experimental data for propylene carbonate in Fig. 3 fit well to this equation with a constant value of $C = 0.126$. The temperature dependence of P_C is shown in the inset of Fig. 3. The equation for the isothermal compressibility, $-\frac{1}{V} \frac{\partial V}{\partial P}|_T = \frac{C}{P_C(T) + P}$, can be integrated to give $V = V_0 \left(1 + \frac{P}{P_C(T)}\right)^{-C}$, where V_0 is a reference volume at zero pressure. Since the activation volume depends on a difference between two volumes, it is convenient to expand $f(x) = (1 + x)^{-C}$ as a Maclaurin series in $x = \frac{P}{P_C(T)}$. For $P < P_C$, this yields $f(x) = 1 - Cx + \frac{C(C+1)}{2!}x^2 - \frac{C(C+1)(C+2)}{3!}x^3 \dots$. Since $C = 0.126$, $\frac{C(C+1)}{2!} = 0.071$ and $\frac{C(C+1)(C+2)}{3!} = 0.050$. We assume that these equations apply to both the initial- and transition-states so that the molar activation volume is $\alpha^* \Delta V_P^\ddagger(P) = \alpha^* (\tilde{V}_T(P) - \tilde{V}_I(P))$. This leads to the final equation for the pressure-dependent activation volume as

$$\alpha^* \Delta V_P^\ddagger(P) = \alpha^* \Delta V_P^{\ddagger 0} - 0.126 \left(\frac{\tilde{V}_T^0}{P_C^T} - \frac{\tilde{V}_I^0}{P_C^I} \right) \alpha^* P + 0.071 \left(\frac{\tilde{V}_T^0}{P_C^{T^2}} - \frac{\tilde{V}_I^0}{P_C^{I^2}} \right) \alpha^* P^2 \dots \quad (16)$$

where $\alpha^* \Delta V_P^{\ddagger 0}$ is the activation volume at zero pressure. The Barus coefficient becomes $\alpha_B(T, P) = \frac{\alpha^* \Delta V_P^\ddagger(P)}{k_B T}$ and is used to calculate the pressure dependence of the activation volume as the system is compressed from ensemble I to ensemble II.

The results are fitted to the low-pressure ($P < 0.6$ GPa) propylene carbonate activation volumes obtained from the viscosity measured at 378 K displayed in Fig. 4. This yields a zero-pressure activation volume, $\alpha^* (\tilde{V}_T^0 - \tilde{V}_I^0) = 1.60 \pm 0.02 \times 10^{-5}$ m³/mol, which is typical of chemical processes.³¹ The fit gives values of $\alpha^* \left(\frac{\tilde{V}_T^0}{P_C^T} - \frac{\tilde{V}_I^0}{P_C^I} \right) = 1.88 \pm 0.16 \times 10^{-13}$ m³/Pa and $\alpha^* \left(\left(\frac{\tilde{V}_T^0}{P_C^{T^2}} - \frac{\tilde{V}_I^0}{P_C^{I^2}} \right) \right) = 3.92 \pm 0.43 \times 10^{-22}$ m³/Pa². The validity of these parameters can be gauged since the value of P_C^I for the initial-state structure is known from the fit to the isothermal compressibility data in Fig. 3, where $P_C^I = 2.08 \times 10^8$ Pa at 378 K. The value of \tilde{V}_I^0 is equal to the molar volume of propylene carbonate (8.70×10^{-5} m³/mol) at zero pressure so that we can calculate a value of $\alpha^* \left(\frac{\tilde{V}_I^0}{P_C^I} \right)$ for the initial state. This depends on α^* , the number of molecules in the low-pressure ensemble (II). This in turn allows the value of $\alpha^* \left(\frac{\tilde{V}_T^0}{P_C^T} \right)$ for the transition-state structure to be obtained from the slope ($1.88 \pm 0.16 \times 10^{-13}$ m³/Pa) of the activation volume vs pressure curve [Fig. 4 and Eq. (16)]. We can similarly calculate not only the value of $\alpha^* \left(\frac{\tilde{V}_I^0}{P_C^I} \right)$ for an ensemble/CRR with α^* molecules but also the value of $\alpha^* \left(\frac{\tilde{V}_T^0}{P_C^T} \right)$ for the transition-state structure from the quadratic dependence of the activation volume ($3.92 \pm 0.43 \times 10^{-22}$ m³/Pa²). The ratio of these two quantities gives

a value of P_C^T , and these results can be used to calculate $\alpha^* \tilde{V}_T^0$ in two different ways: (i) from the zero-pressure activation volume, $\alpha^* (\tilde{V}_T^0 - \tilde{V}_I^0) = 1.60 \pm 0.02 \times 10^{-5}$, and (ii) by substituting the value of P_C^T into the equation for the slope of the activation volume vs pressure curve, $\alpha^* \left(\frac{\tilde{V}_T^0}{P_C^T} \right) = \alpha^* \left(\frac{\tilde{V}_I^0}{P_C^I} \right) - 1.92 \pm 0.2 \times 10^{-14}$ m³/Pa. Both results depend on α^* . To determine the best value of α^* , it was systematically varied until identical values of $\alpha^* \tilde{V}_T^0$ were obtained by both methods, which occurred at $\alpha^* \sim 15 \pm 3$ molecules. The calculation also yielded the molar volume of the transition-state structure, $\tilde{V}_T^0 = 88.1 \pm 0.2$ cm³/mol, slightly larger than the molar volume of the initial-state of propylene carbonate (87.0 cm³/mol), as expected. The resulting value of P_C^T (0.211 GPa) is also only slightly different from that of 0.208 GPa for the undistorted propylene carbonate, P_C^I . This suggests that the ensemble/CRR structure is only slightly perturbed when molecular exchange occurs, thus justifying the assumption made above that $\left(\frac{z_T(T)}{z_I(T)} \right) \sim 1$. Thus, these results are in accord with the idea that the whole, three-dimensional CRR present at low pressures contains about 13 molecules. Note that structure III formed at higher pressures when the CRRs start to grow is likely to be much less compliant than these low-pressure structures and the activation volume will then be dominated by the growth of the CRRs.

VII. THE VISCOSITY OF GLASS-FORMING FLUIDS USING ADAM-GIBBS THEORY

The next task is to calculate a value of α^* at higher pressures and lower temperatures (ensemble III in Fig. 5) in the region where they are expected to grow to eventually form a glassy structure. It is clear from the results in Fig. 4 that the low-pressure decrease in activation volume is due to the compressibility of the molecular ensemble below ~ 0.3 – 0.4 GPa, but the activation volume then starts to increase at higher pressures. It is proposed that this is due to a compression of the low-pressure CRR (ensemble I) as described in Sec. IV until there is little vacant space (free volume) between molecules for them to change positions. At higher pressures, molecules can exchange positions only by more of the surrounding molecules moving to make space available. Any increase in the size of the CRR increases both the activation volume, $\alpha^*(T, P) \Delta V_P^\ddagger$, and the activation barrier because they both scale with α^* .

The task is then to calculate the pressure dependence of $\alpha^*(T, P)$, which is accomplished by using Adam-Gibbs theory. According to Ehrenfest, at a second-order transition from a liquid to a solid at a temperature T_2 , the entropy, volume, and free energy are continuous functions of temperature, while the specific heat capacity, thermal expansion coefficient, and compressibility are discontinuous. Thus, as a liquid cools to form a solid, it must become more ordered, thus requiring the constituent molecules to move to take up the locations in the solid lattice, thereby reducing its entropy. Adam-Gibbs theory shows how the rate of that process depends on the difference in configurational entropy between the solid and liquid phases. Thus, there is a significant relaxation-time increase as a consequence of the approach to the phase transition that implies that the rate at which the molecules can reorganize becomes slow on a laboratory time scale, resulting in the formation of a glass at a higher temperature, T_g . As a result, the glass-transition

temperature is not a thermodynamically defined quantity but rather depends on the cooling rate. For example, metals can be persuaded to form glasses if they are cooled sufficiently rapidly.⁶⁹

The configurational entropy of a system in which the probability of occurrence of the i th configuration is p_i is given by the Boltzmann equation, $\langle k_B \ln p_i \rangle$, where $\langle \dots \rangle$ represents an average over all configurations. The CRR must be one of these configurations. The configurational entropy of an individual CRR shown in Fig. 5, where a blue molecule exchanges with an orange one to give two identical configurations, is $s_C^* = k_B \ln 2$. Different numbers of exchanging molecules in the ensemble are, in principle, possible, which would give correspondingly larger values of s_C^* . If, at any given temperature and pressure, there are a total of L CRRs, each containing α^* molecules, then the total number of molecules in the system $N = L\alpha^*$. The total configurational entropy of the system is obtained by summing over all possible CRRs: $S_C = \sum_{i=1}^L \langle k_B \ln p_i \rangle$. However, the principle of equal *a priori* probability indicates that each configuration is equally probable and equal to s_C^* . Thus, $S_C = \sum_{i=1}^L s_C^* = Ls_C^*$ so that the average number of CRRs is given by $L = S_C/s_C^*$. Now, substituting for L from the above-mentioned expression, the final equation for the average number of molecules in a CRR for one mole of material ($N = N_A$, Avogadro's number) is

$$\alpha^*(T, P) = N_A \frac{s_C^*}{S_C(T, P)}. \quad (17)$$

Thus, as the temperature decreases, the number of molecules in the CRR increases so that, in principle, at the second-order transition temperature, the number of molecules in CRR becomes close to infinite as it forms a solid. However, as noted above, the rate becomes very small at the glass-transition temperature, T_g , often about 50 K above T_2 , where the CRR contains a finite number of molecules.

Substituting Eq. (17) into Eq. (9) gives the following expression for how the molecular exchange rate, $\bar{k}(T, P)$, depends on the configurational entropy:

$$\bar{k}(T, P) = \bar{k}_0 \exp \left(-\frac{N_A s_C^* (E^\ddagger + P\Delta V^\ddagger)}{S_C(T, P) k_B T} \right). \quad (18)$$

Note that Eq. (9) is quite general and does not presume a specific value of α^* but just describes the consequence of the assumption that a minimum ensemble size is required to allow molecular exchange to occur.¹³

The final task is to obtain the temperature and pressure dependences of S_C . As shown in Sec. III, the entropy of the liquid includes contributions from both the one-particle partition function and from the configuration so that the liquid entropy can be written as $S^l = S_{internal}^l + S_C$. By definition, the configurational entropy of a perfect solid is zero so that the entropy of the solid is $S^s = S_{internal}^s$. If it is assumed that $S_{internal}^l \sim S_{internal}^s$, that is, their one-particle partition functions are similar, then $S_C = S^l - S^s$, which becomes zero at T_2 ($S^l = S^s$) and remains zero at lower temperatures. The temperature dependence of the configurational entropy of propylene carbonate has been calculated¹³ based on data from Tatsumi *et al.*⁷⁰ The resulting values of S_C are plotted as a function of temperature in Fig. 6 and can be fit very well to an empirical function of the form $S_C = \beta(1 - \frac{T_0}{T})$, which equals zero at $T = T_0$ and yields a value of ~ 137 K, close to the Kauzmann temperature of propylene carbonate

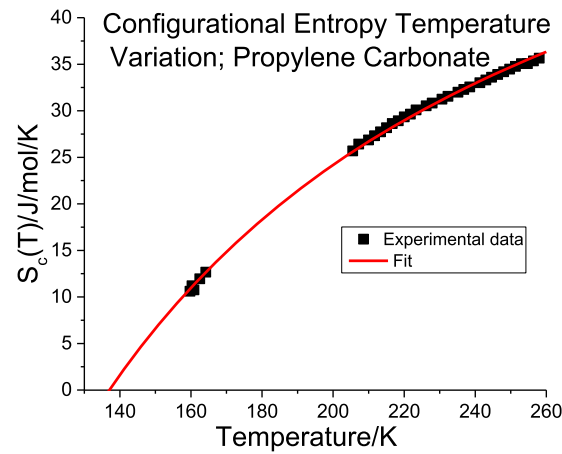


FIG. 6. Plot of S_C as a function of temperature for propylene carbonate obtained from measurements of C_P vs temperature (see the text). The line is a fit to the empirical formula $S_C = \beta(1 - \frac{T_0}{T})$, where T_0 is the temperature at which the configurational entropy goes to zero. The fit yields $\beta = 76.9 \pm 0.3$ J/mol/K and $T_0 = 137.0 \pm 0.3$ K. Reproduced with permission from M. Ozawa *et al.*, J. Chem. Phys. **151**, 084504 (2019). Copyright 2024 AIP Publishing LLC.

of ~ 126 K,⁷¹ although this is formally the second-order transition temperature, T_2 . Note, however, that the value of limiting temperature obtained below from fits to the pressure-dependent activation energy is significantly higher than that measured here from the variation in configurational entropy with temperature. Various values have been suggested for the glass-transition temperature from ~ 220 ⁷² to 169 K,⁷³ reflecting the fact that it depends on the kinetics of the system. Accordingly, we will consider T_0 to be a fitting parameter and defer discussions of its physical meaning for later. Substituting the fit in Fig. 6 into Eq. (18) gives

$$\begin{aligned} \bar{k}(T, P) &= \bar{k}_0 \exp \left(-\frac{N_A s_C^* (E^\ddagger + P\Delta V^\ddagger)}{\beta k_B (T - T_0(P))} \right) \\ &= \bar{k}_0 \exp \left(-\frac{N_A s_C^* E^\ddagger}{\beta k_B (T - T_0(P))} \right) \exp \left(-\frac{N_A s_C^* P\Delta V^\ddagger}{\beta k_B (T - T_0(P))} \right), \end{aligned} \quad (19)$$

which gives a formula for the temperature variation in the rate that is in accord with the Vogel–Fulcher–Tammann (VFT) equation.

The activation energies have been measured for propylene carbonate viscosity,¹ and the results are shown in Fig. 7. This shows that the pressure dependences are higher at lower temperatures, consistent with them having larger CRRs. According to the above-mentioned analysis, the activation energy should vary with temperature and pressure as $E_{act} = \frac{N_A s_C^* E^\ddagger}{\beta(1 - T_0(P)/T)}$.

The results in Fig. 7 were fit to $E_{act} = \frac{E_0^\ddagger}{(1 - T_0(P)/T)}$ at each pressure to give values of $T_0(P)$ and $E_0^\ddagger(P)$, where $E_0^\ddagger = \frac{N_A s_C^* E^\ddagger}{\beta}$, which, according to the assumptions of Adam and Gibbs, should be constant if E^\ddagger is constant and if the entropy model correctly predicts the growth of the CRRs.

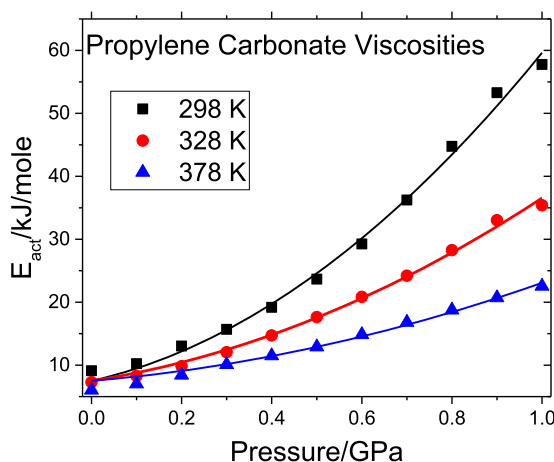


FIG. 7. Plot of the activation energy for the viscosity of propylene carbonate for various temperatures as a function of pressure up to a maximum of 1 GPa. Reproduced from R. Casalini and S. Bair, *J. Chem. Phys.* **128**, 084511 (2008). Copyright 2008 AIP Publishing LLC.

The resulting values of $T_0(P)$ are plotted as a function of pressure in Fig. 8. The low-pressure limit of the critical temperature is $T_0 \sim 213$ K, close to the value obtained from Fig. 6 based on the specific heat capacity, implying that T_0 remains constant up to ~ 0.3 GPa, where the ensembles do not change in size. The linear portion at higher pressures has a slope of ~ 80 K/GPa, due to a variation in T_0 with pressure, but then stabilizes at ~ 0.8 GPa at a value of ~ 260 K.

Figure 9 displays the corresponding variation in the value of E^\ddagger as a function of pressure, which varies linearly from ~ 2.5 kJ/mol at zero pressure to ~ 7 kJ/mol at 1 GPa. These results suggest that, while the Adam-Gibbs model captures the broad trends in the high-pressure viscosity of propylene carbonate (see Fig. 10), other effects,

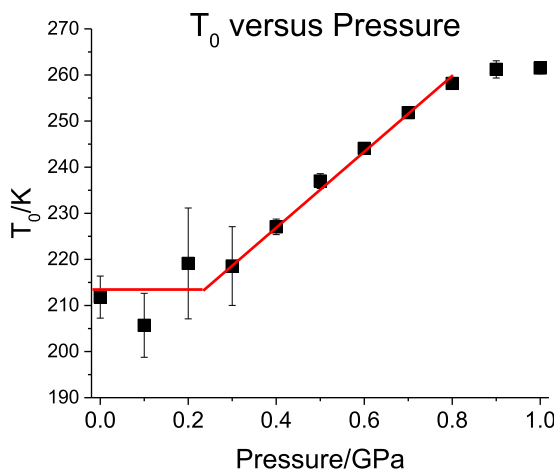


FIG. 8. Plot of the critical temperature in the Adam-Gibbs model for the viscosity of propylene carbonate as a function of pressure up to a maximum of 1 GPa.

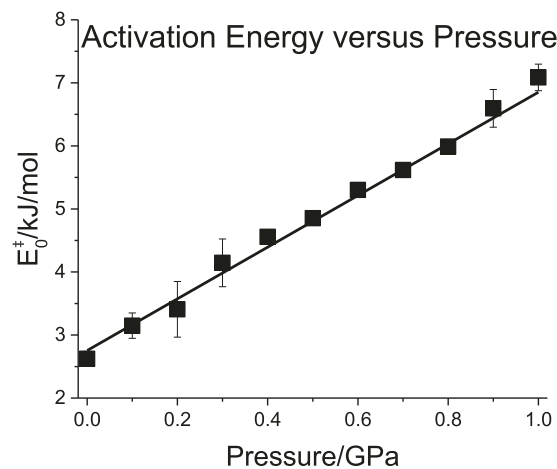


FIG. 9. Plot of the activation energy in the Adam-Gibbs model for the viscosity of propylene carbonate as a function of pressure up to a maximum of 1 GPa.

which are not included in the model, also seem to contribute. This difference might also influence the calculated values of T_0 . The activation energy per molecule E^\ddagger in the CRR is assumed to be a constant in the Adam-Gibbs model, but it is found to increase linearly with pressure in these experiments. This is perhaps not surprising given that Adam-Gibbs describes an entropy-based model, which assumes that the energy also scales with the number of molecules in the CRR. These results suggest that this is an oversimplification but can be corrected empirically by adding a simple linear pressure-dependent energy to the model.

The activation volume at higher pressures is reasonably modeled by assuming that the critical temperature in the Adam-Gibbs

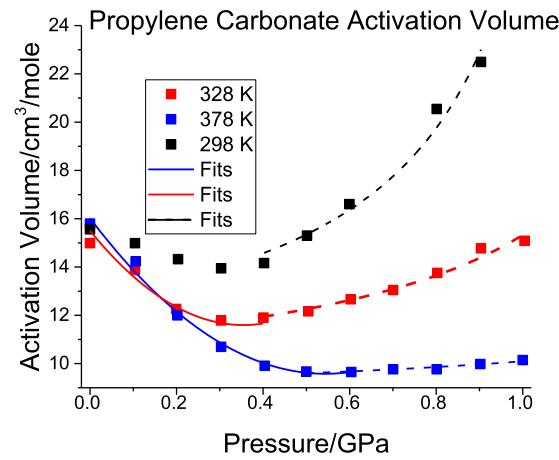


FIG. 10. Variation in the viscosity activation volume as a function of pressure for different fluid temperatures. The dashed line shows the fit of $\frac{D}{T-\beta(P+P_0)}$ to the activation volume V_{act} for pressures above ~ 0.4 GPa. Reproduced with permission from R. Casalini and S. Bair, *J. Chem. Phys.* **128**, 084511 (2008). Copyright 2008 AIP Publishing LLC.

model varies linearly with pressure (Fig. 8). Indeed, a thermodynamic analysis of the theoretical behavior of $\frac{dT_2}{dP}$ indicates that it depends on the isobaric expansion coefficient, $\alpha_T = \frac{1}{V} \frac{\partial V}{\partial T}|_P$, and the isothermal compressibility to give $\frac{dT_2}{dP} = \frac{\Delta\kappa}{\Delta\alpha}|_{T=T_2}$ at the second-order transition temperature T_2 , where $\Delta\kappa$ and $\Delta\alpha$ are the compressibility and thermal expansion coefficient changes between the liquid and solid states at T_2 . Hence, T_2 is expected to change linearly with pressure. The isothermal compressibility follows the Tait equation above T_2 , $\kappa_T = \frac{C}{P_C(T) + P}$, and the fits are shown in Fig. 3, where $C = 0.126 \pm 0.007$ and is independent of temperature and $P_C(T)$ varies between 0.2 and 0.3 GPa (see the inset of Fig. 3). Note that these values were used to calculate the variation in activation volume with pressure in Sec. VI. While the thermal expansion coefficient of propylene carbonate of the liquid has been measured,⁷⁴ to the best of the author's knowledge, it has not been reported for the glass phase, and hence, a calculation of $\Delta\alpha$ is not possible.

The general picture of the variation in activation volume for pressures above ~ 0.3 GPa is consistent with there being a pressure-dependent number of molecules in the ensemble that makes up the CRR. Equation (19) predicts that the effective activation volume should vary as $1/(T - T_0(P))$. From the results shown in Fig. 8, at a pressure of ~ 0.3 GPa where $T_0 = 215$ K, $(T - T_0(P))$ varies from 158 to 108 to 78 K for data collected at 378, 328, and 298 K (Fig. 10), but $(T - T_0(P))$ reduces to 118, 68, and 38 K at 1 GPa, consistent with the experimental variation in activation volume. Figure 8 shows that T_0 varies linearly with pressure over the range at which Adam–Gibbs theory is proposed to operate so that $T_0 = \gamma(P + P_0)$, where, from Fig. 8, $\gamma = 82.4 \pm 0.2$ K/GPa and $P_0 = 2.36$ GPa. This implies that, for pressures above ~ 0.3 GPa, the activation volume should depend on pressure as $\Delta V^\ddagger = \frac{D}{T - \gamma(P + P_0)}$.

This equation was fitted to the high-pressure experimental data for the activation volume, and the results are shown as dashed lines in Fig. 10. The fits to the above-mentioned formula agree well with experiment and, in particular, reproduces the non-linearity found at the lowest temperature. This indicates that the results at higher pressures are due to the formation of larger CRR ensembles that grow more quickly with pressure at lower temperatures. This analysis of the variation in fluid viscosity over a wide range of pressures and for several temperatures provides insights into the nature of the cooperatively rearranging region proposed by Adam and Gibbs. It also allows the identification of the extent to which the assumptions made by Adam and Gibbs impact the accuracy of the model and will guide future efforts to improve the accuracy of the model.

VIII. SUMMARY

The pressure dependence of the activation volume of a glass-forming fluid, propylene carbonate, initially decreases as the pressure increases, but then starts to increase at higher pressures with a value and slope that depend on the temperature (Fig. 4). The general behavior is analyzed using Evans–Polanyi perturbation theory considering the pressure-dependent structural evolution depicted in Fig. 5. The idea is that the structural changes that occur when the fluid is compressed at a particular temperature modify the rate at which a molecule in the fluid can diffuse through it. It is also assumed that the rate of molecular transport controls various phenomena such as the fluid relaxation time, its viscosity, and the rate

at which the structure transforms as the fluid is cooled to form metastable structures, i.e., glasses. At low pressures, the liquid is moderately disordered with sufficient space between the molecules (large free volume) to facilitate molecular motion from one site to the next as shown in structure I in Fig. 5. Structure I is relatively compressible (Fig. 3) with a compressibility that increases with increasing temperature. The molecular ensemble that allows molecules to change places in the fluid remains constant and is similar to that suggested by Alfrey except that we assume that the exchange occurs between a central molecule and one of its nearest neighbors. This situation can be analyzed using Eyring's viscosity model but implemented using Evans–Polanyi perturbation theory. The conversion to Newtonian viscosity at lower pressures and the decrease in activation volume with increasing pressure are ascribed to a change in the Barus coefficient as the intermolecular spacing decreases. This is accompanied by a modest increase in the activation energy. Such pressure-dependent activation volumes have been analyzed for chemical reactions,³¹ where, because of the relatively large activation energies, the influence of changes in activation volume with pressure is negligible, while they become significant for lower-barrier processes such as molecule exchange. As such, we expect this effect to be a common feature of fluid viscosity.

When the pressure increases above ~ 0.2 GPa, the compressibility becomes smaller and less temperature dependent and the molecules interact to cause Pauli repulsion to form ensemble II (Fig. 5). Now, the molecules are sufficiently crowded that there is insufficient space in the Thomas-like structure for molecules to exchange, and this requires more molecules to be able to move to provide sufficient space for exchange with another molecule; the CRR is forced to grow. This leads to a temperature-dependent inflection point in the plot of activation volume vs pressure at the point at which ensemble II is formed.

The growth in CRR is analyzed using Adam–Gibbs theory but modified by using the Evans–Polanyi approach to calculate the molecular transport rate and the pressure-dependent viscosity. Note, however, that the physical processes that underpin this effect are rooted in concepts of free-volume theory. While this model provides general agreement between theory and experiment, there are crucial differences. First, both the activation energies and the activation volumes increase with pressure, while Adam–Gibbs theory proposes that the energy per molecule should remain constant. Second, in the case of propylene carbonate, the critical temperature, T_0 , does not seem to coincide with the temperature of the second-order phase transition, T_2 . The difference will guide strategies for improving the model. Finally, Casalini and Bair pointed out that there is an inverse correlation between the pressure-dependent activation energy (Fig. 9) and the isothermal compressibility (Fig. 3).¹ This inverse correlation is justified by the structural evolution model proposed here.

ACKNOWLEDGMENTS

We acknowledge the Civil, Mechanical and Manufacturing Innovation (CMMI) Division of the National Science Foundation under Grant Nos. 2020525 and 262 and the Chemical, Bioengineering, Environmental and Transport (CBET) Division under Grant No. 16609 for support of this work. We also thank Dr.

Michael Moseler of the Fraunhofer Institute for Mechanics of Materials, Freiburg and James Ewen of Imperial College, London, for extremely useful discussions. Finally, we thank one reviewer for carrying out experiments to check the isothermal compressibility results.

AUTHOR DECLARATIONS

Conflict of Interest

The authors have no conflicts to disclose.

Author Contributions

Nicholas Hopper: Formal analysis (equal); Writing – review & editing (equal). **Rosa M. Espinosa-Marzal:** Formal analysis (equal); Validation (equal); Writing – review & editing (equal). **Wilfred Tysoe:** Conceptualization (equal); Formal analysis (equal); Project administration (equal); Writing – original draft (equal).

DATA AVAILABILITY

The data support the findings of this study are available from the corresponding author upon reasonable request.

REFERENCES

- ¹R. Casalini and S. Bair, *J. Chem. Phys.* **128**, 084511 (2008).
- ²S. Pawlus *et al.*, *Phys. Rev. E* **70**, 061501 (2004).
- ³M. Ozawa *et al.*, *J. Chem. Phys.* **151**, 084504 (2019).
- ⁴S. Bair *et al.*, *Tribol. Lett.* **58**, 16 (2015).
- ⁵H. Spikes and J. Zhang, *Tribol. Lett.* **58**, 17 (2015).
- ⁶R. Byron Bird and P. J. Carreau, *Chem. Eng. Sci.* **23**, 427 (1968).
- ⁷H. Eyring, *J. Chem. Phys.* **4**, 283 (1936).
- ⁸W. Kauzmann and H. Eyring, *J. Am. Chem. Soc.* **62**, 3113 (1940).
- ⁹J. P. Ewen, H. A. Spikes, and D. Dini, *Tribol. Lett.* **69**, 24 (2021).
- ¹⁰M. L. Williams, R. F. Landel, and J. D. Ferry, *J. Am. Chem. Soc.* **77**, 3701 (1955).
- ¹¹M. H. Cohen and D. Turnbull, *J. Chem. Phys.* **31**, 1164 (1959).
- ¹²P. B. Macedo and T. A. Litovitz, *J. Chem. Phys.* **42**, 245 (1965).
- ¹³M. Goldstein, *J. Chem. Phys.* **51**, 3728 (1969).
- ¹⁴E. Orowan, *Proceedings of the First U.S. National Congress of Applied Mechanics* (ASME, 1952).
- ¹⁵G. Adam and J. H. Gibbs, *J. Chem. Phys.* **43**, 139 (1965).
- ¹⁶T. Alfrey, *Rheol. Bull.* **16**, 5 (1945).
- ¹⁷J. Hirschfelder, D. Stevenson, and H. Eyring, *J. Chem. Phys.* **5**, 896 (1937).
- ¹⁸C. Barus, *Am. J. Sci.* **s3-45**, 87 (1893).
- ¹⁹L. Xing *et al.*, *Acc. Chem. Res.* **51**, 282 (2018).
- ²⁰N. Yao *et al.*, *Angew. Chem., Int. Ed.* **62**, e202305331 (2023).
- ²¹J. Barthel and F. Feuerlein, *J. Solution Chem.* **13**, 393 (1984).
- ²²P. W. Bridgman, *Proc. Am. Acad. Arts Sci.* **61**, 57 (1926).
- ²³S. Bair, *Sci. Rep.* **12**, 3422 (2022).
- ²⁴M. G. Evans and M. Polanyi, *Trans. Faraday Soc.* **31**, 875 (1935).
- ²⁵M. G. Evans and M. Polanyi, *Trans. Faraday Soc.* **32**, 1333 (1936).
- ²⁶M. G. Evans and M. Polanyi, *Trans. Faraday Soc.* **34**, 11 (1938).
- ²⁷A. Boscoboinik *et al.*, *Chem. Commun.* **56**, 7730 (2020).
- ²⁸R. Rana *et al.*, *Tribol. Lett.* **69**, 32 (2021).
- ²⁹N. Hopper *et al.*, *Phys. Chem. Chem. Phys.* **25**, 15855 (2023).
- ³⁰N. Hopper *et al.*, *Tribol. Lett.* **71**, 121 (2023).
- ³¹N. Hopper *et al.*, *RSC Mechanochem.* **1**, 402 (2024).
- ³²R. Rana *et al.*, *Tribol. Lett.* **72**, 76 (2024).
- ³³S. S. M. Konda *et al.*, *J. Chem. Phys.* **135**, 164103 (2011).
- ³⁴L. D. Landau and E. M. Lifshitz, in *Statistical Physics*, 3rd ed., edited by L. D. Landau and E. M. Lifshitz (Butterworth-Heinemann, Oxford, 1980), p. 333.
- ³⁵A. K. Doolittle, *J. Appl. Phys.* **22**, 1471 (1951).
- ³⁶A. K. Doolittle and D. B. Doolittle, *J. Appl. Phys.* **28**, 901 (1957).
- ³⁷P. G. Tait, *Report on Some of the Physical Properties of Fresh Water and of Sea Water* (Johnson Reprint Corporation, 1965).
- ³⁸T. L. Hill, *An Introduction to Statistical Thermodynamics* (Dover Publications, Newburyport, 2012).
- ³⁹H. Eyring, *J. Chem. Phys.* **3**, 107 (1935).
- ⁴⁰G. I. Bell, *Science* **200**, 618 (1978).
- ⁴¹T. Asano and W. J. Le Noble, *Chem. Rev.* **78**, 407 (1978).
- ⁴²A. Drjaca *et al.*, *Chem. Rev.* **98**, 2167 (1998).
- ⁴³G. Subramanian, N. Mathew, and J. Leiding, *J. Chem. Phys.* **143**, 134109 (2015).
- ⁴⁴D. E. Makarov, *J. Chem. Phys.* **144**, 030901 (2016).
- ⁴⁵S. M. Avdoshenko and D. E. Makarov, *J. Phys. Chem. B* **120**, 1537 (2016).
- ⁴⁶G. Henkelman, B. P. Uberuaga, and H. Jonsson, *J. Chem. Phys.* **113**, 9901 (2000).
- ⁴⁷G. Henkelman and H. Jónsson, *J. Chem. Phys.* **113**, 9978 (2000).
- ⁴⁸G. Henkelman, G. Jóhannesson, and H. Jónsson, in *Theoretical Methods in Condensed Phase Chemistry*, edited by S. D. Schwartz (Springer Netherlands, Dordrecht, 2002), p. 269.
- ⁴⁹B. Peters, in *Reaction Rate Theory and Rare Events Simulations*, edited by B. Peters (Elsevier, Amsterdam, 2017), p. 183.
- ⁵⁰R. Hill, *J. Mech. Phys. Solids* **16**, 229 (1968).
- ⁵¹E. Thoms *et al.*, *J. Phys. Chem. Lett.* **9**, 1783 (2018).
- ⁵²P. W. Bridgman, *Proc. Am. Acad. Arts Sci.* **77**, 117 (1949).
- ⁵³R. L. Cook *et al.*, *J. Chem. Phys.* **100**, 5178 (1994).
- ⁵⁴H. Vogel, *Phys. Z.* **22**, 645 (1921).
- ⁵⁵G. S. Fulcher, *J. Am. Ceram. Soc.* **8**, 339 (1925).
- ⁵⁶G. Tammann and W. Hesse, *Z. Anorg. Allg. Chem.* **156**, 245 (1926).
- ⁵⁷D. L. Hogenboom, W. Webb, and J. A. Dixon, *J. Chem. Phys.* **46**, 2586 (1967).
- ⁵⁸T. Odagaki, *J. Phys. Soc. Jpn.* **91**, 043602 (2022).
- ⁵⁹J. D. Stevenson, J. Schmalian, and P. G. Wolynes, *Nat. Phys.* **2**, 268 (2006).
- ⁶⁰R. E. Powell, W. E. Roseveare, and H. Eyring, *Ind. Eng. Chem.* **33**, 430 (1941).
- ⁶¹J. E. Mayer and E. Montroll, *J. Chem. Phys.* **9**, 2 (1941).
- ⁶²F. Rizk *et al.*, *Phys. Rev. Lett.* **129**, 074503 (2022).
- ⁶³H. Gao and M. H. Müser, *Tribol. Lett.* **72**, 16 (2023).
- ⁶⁴A. E. Stearn and H. Eyring, *Chem. Rev.* **29**, 509 (1941).
- ⁶⁵J. F. Kincaid, H. Eyring, and A. E. Stearn, *Chem. Rev.* **28**, 301 (1941).
- ⁶⁶M. Cukierman, J. W. Lane, and D. R. Uhlmann, *J. Chem. Phys.* **59**, 3639 (1973).
- ⁶⁷K. L. Johnson and J. L. Tevaarwerk, “Shear behaviour of elastohydrodynamic oil films,” *Proc. R. Soc. London, Ser. A* **356** (1685), 215 (1977).
- ⁶⁸E. Bou-Chakra *et al.*, *Tribol. Int.* **43**, 1674 (2010).
- ⁶⁹A. Takeuchi and A. Inoue, *Mater. Sci. Eng.: A* **304-306**, 446 (2001).
- ⁷⁰S. Tatsumi, S. Aso, and O. Yamamuro, *Phys. Rev. Lett.* **109**, 045701 (2012).
- ⁷¹H. Fujimori and M. Oguni, *J. Chem. Thermodyn.* **26**, 367 (1994).
- ⁷²V. Pokorný *et al.*, *J. Chem. Eng. Data* **62**, 4174 (2017).
- ⁷³T. Eisenbach *et al.*, *J. Phys. Chem. Ref. Data* **50**, 023105 (2021).
- ⁷⁴P. Lunkenheimer *et al.*, *Nat. Phys.* **19**, 694 (2023).